applied optics

Vector magnetometer based on the effect of coherent population trapping

V. Andryushkov, D. Radnatarov, and S. Kobtsev*

Division of Laser Physics and Innovative Technologies, Novosibirsk State University, Novosibirsk, 630090, Russia
**Corresponding author: sergey.kobtsev@gmail.com*

Received 24 February 2022; revised 27 March 2022; accepted 28 March 2022; posted 5 April 2022; published 21 April 2022

The method is presented for converting a coherent population trapping (CPT) atomic clock into a CPT vector (compass-) magnetometer without mechanically moving parts through a relatively simple add-on. The system of 3D Helmholtz coils was used for compensation of the external magnetic field, allowing measurement of both strength and direction of a magnetic field at the sensitivity level of sub−nT/Hz$^{1/2}$ within a 10-Hz bandwidth. Angular resolution of the developed vector magnetometer amounts to about 10^{-2} degrees.

https://doi.org/10.1364/AO.457087

1. INTRODUCTION

The functional similarity of the physical principles of operation between quantum frequency standards and quantum magnetometers results in any progress made in one of these fields immediately reflected in the other. For example, the development of a miniaturized atomic clock based on coherent population trapping (CPT) [1,2] led to the introduction of an atomic magnetometer relying on the same effect [3–5]. The primary difference between the clock and the magnetometer is that in the atomic clock, the reference CPT resonance is excited on magnetically insensitive transitions between the energy levels of hyperfine structure (HFS) in alkali metal atoms, thus ensuring the highly stable spectral position of the resonance [6,7]. In contrast, in atomic magnetometers, sublevel transitions are used that undergo a Zeeman shift in an external magnetic field [8]. One of the drawbacks of such a magnetometer is that, generally, only the absolute strength of the magnetic field is measured and not its spatial components, which would be necessary to determine the direction of the field. Various methods are conventionally used to measure the direction of the magnetic field, of which the simplest involve mechanical movement of the entire magnetometer [9] or some of its parts [10]. However, mechanical motion is not the preferred way of modern research and development. An alternative approach would be creating an ultra-sensitive atomic three-axis chip-scale magnetometer free of any mechanically displaced parts or, in more basic implementation, a magnetic gradiometer/variometer [11]. Realizing a three-axis magnetometer free of mechanical motion is practically possible, but requires either more complicated polarization techniques, nonlinear magneto-optical rotation, a multi-pass cell, or based on modeling only [12–15]; and/or it may necessitate a system of compensation solenoids [16–20]. Similar (compensation) solenoid coils have also been sometimes used in scalar CPT magnetometers without μ-metal shielding for compensation of external stationary magnetic fields [21].

Earlier on, this approach was applied both to measurement of the strength and direction of stationary or slowly varying magnetic fields on the basis of the Hanle effect [16], in which a resonance in transmitted radiation is observed at complete cancellation of the external field and to the Mx configuration [17] where the magneto-optical resonance is excited in an optically pumped medium by RF radiation at the Larmor frequency. Application of compensation coils has allowed development of vector atomic spin-exchange relaxation free magnetometers, designed according to the pump–probe [18] and single-beam configurations [19,20]. Thus, it was earlier demonstrated that the compensation approach can be used for measurement of the magnetic field along three axes. We found it promising to implement this idea in a compact device on the basis of a CPT atomic clock.

This year, virtually at the same time, the idea of making a magnetometer on the basis of a CPT atomic clock by addition of electromagnetic coils for compensation of the external magnetic field in order to keep the spectral position of the CPT resonance constant was demonstrated in [22,23]. These works differ in that one of them (written by the authors of the present article) [22] employs this approach to develop a vector magnetometer, whereas the other [23] uses an analogous one to create a scalar magnetometer with an attempt to make it compact. The demonstrated sensitivities of magnetic strength measurement are quite close in both cases at around 300 pT/Hz$^{1/2}$. The possibility in principle to build a vector magnetometer using this approach was proven somewhat later in [24], but in that publication no data are provided about the achieved sensitivity. Furthermore, the experiment discussed in [24] was conducted on the basis of a relatively large optical

cell (∅25.4 mm × 50 mm), that is why work [24] cannot be called a practical demonstration of conversion of commercial (or small-footprint) CPT atomic clocks into CPT magnetometers.

The effect of magnetic field deviation upon the amplitude of CPT resonances has long been discovered [4]. It was not, however, known how precisely this effect may be used for measurement of magnetic field direction, neither has this effect been actually used in practice for this purpose. As the studies presented in the following demonstrate, this dependence can be used for precise measurement of the magnetic field direction.

In the present work, a system of compensation-modulation magnetic coils was used, to our knowledge, for the first time for conversion of a CPT-based laboratory small-footprint atomic clock [25,26] (or commercial CPT atomic clock) into an atomic vector magnetometer. The advantage of this configuration is that many atomic clock components may be used without modification. CPT-based atomic frequency standards have advanced to very compact dimensions, and they may be also very light and consume little energy. If the magnetic shield of an atomic clock is replaced with a system of external magnetic field compensation (compact 3D coils around the optical cell), one obtains a configuration for vector measurement of magnetic field that conserves all the advantages of a CPT-based atomic clock: compact dimensions, low energy consumption, and light weight. The aim of the present work is the study of a vector magnetometer fabricated from unmodified components of a CPT atomic clock.

2. EXPERIMENT

The principle of the proposed compensation vector CPT magnetometer consists in the following: a special stationary magnetic field is created around the optical cell with the help of three-axis Helmholtz coils. Our work did not aim to demonstrate the smallest possible size of the device. The magnetometer's dimensions were relatively small and close to those of commercial CPT clocks. For illustration, we added a photo of self-fabricated Helmholtz coils (Fig. 1) (which could have been made yet slightly smaller). The typical size of the coils may be judged by comparison with a coin placed beside. The optical cell size was ∅8 mm × 5 mm, and that of the coil frame was $35 \times 35 \times 35\ \text{mm}^3$.

It is also necessary to make a clarification of the employed terminology: in this work we chose to utilize the term "CPT magnetometer," even though sometimes such devices are called "coupled dark state magnetometer" [27].

The current flowing within the coils is determined by taking into consideration these factors: the magnitude of the CPT resonance depends [28] upon the presence of the magnetic field component orthogonal to the laser beam, while the spectral position of the CPT resonance is governed by the strength of the magnetic field. Compensation of the external magnetic field was done with the three-axis Helmholtz coils considering this duality of the effects produced by the direction of the magnetic field. Correspondingly, as the first step, the magnitude of the CPT resonance is maximized (since this magnitude reaches its maximum in the absence of the magnetic field component orthogonal to the laser beam). That is, two pairs of Helmholtz coils whose axes are normal to the laser beam are used to cancel

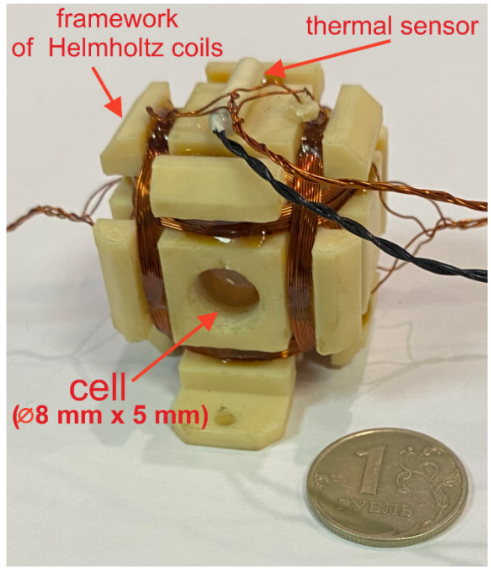

Fig. 1. Self-fabricated Helmholtz coils on a 3D-printed frame.

out the magnetic field component orthogonal to the beam. Operation of two pairs of these coils cancels out both components of the external field orthogonal to the laser beam. The presence of the third field component parallel to the beam does not affect the magnitude of the CPT resonance but modifies its spectral position. Compensation of the third magnetic field component (parallel to the laser beam) is done by attaining a stationary position of the CPT resonance. Therefore, the principle of error signal formation is different for the coils that generate compensating fields respectively parallel and orthogonal to the beam. Compensation of all three magnetic field components may be performed electronically via three feedback loops operating on different aliquant frequencies. This technique of vector CPT magnetometry has been proposed here for the first time.

The proposed approach consists of simultaneous compensation of the external field by a magnetic coil system used to maintain constant magnitude and spectral position of a CPT resonance (^{87}Rb) and achievement of comparatively high device sensitivity. The measured sensitivity of the developed atomic magnetometer amounted to $300\ \text{pT}/\text{Hz}^{1/2}$ within a 10-Hz bandwidth for components normal to the laser beam and $400\ \text{pT}/\text{Hz}^{1/2}$ within the same bandwidth for the magnetic field component parallel to the laser beam.

Figure 2 describes the experimental setup of the studied CPT vector magnetometer. The radiation source used was a vertical-cavity surface-emitting laser (VCSEL) (795 nm). The injection current of the laser was modulated at the frequency equal to half the frequency of the hyperfine splitting $f_{RF} = \nu_{hfs}/2 = 3.417\ \text{GHz}$ using a frequency synthesiser. Thus, the first-order sidebands of the radiation spectrum excited the CPT resonance. The radiation was collimated by passing through a lens and acquired circular polarization passing through a quarter-wave plate ($\lambda/4$). Next, the radiation passed through a cylindrical cell filled with 87Rb vapor. This cell was fabricated according to the cold optical contact technology and had the following internal dimensions: length of 5 mm and diameter of 4 mm. The composition and pressure of the buffer gas mix were optimized for the working temperature

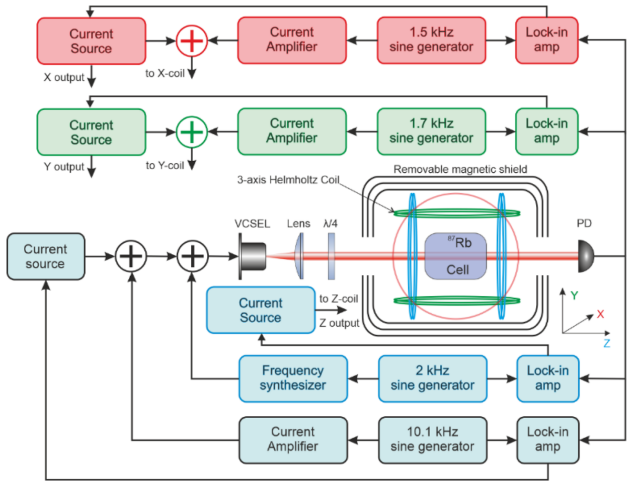

Fig. 2. Experimental setup.

of 70°C [29]. The cell was placed into an aluminum holder heated with a thermoelectric cooler (TEC) inside a multi-layer magnetic screen. The cell temperature was measured by means of a 10−kΩ platinum thermo-resistor, also placed inside the magnetic screen. The vapor-cell was placed inside three-axis Helmholtz coils. The system of three Helmholtz coils was self-made: the coils were wound with copper wire on a frame fabricated with a consumer-grade 3D polymer printer. The coil system and the optical cell were located inside a removable magnetic shield. This made it possible to perform calibration with the magnetic shield on and to measure the vector of the external magnetic field without it. The photodetector measured the transmitted radiation. To stabilize the laser current on the Rb absorption line, a lock-in amplifier was used at the frequency of 10.1 kHz.

The relationship between the current flowing through the Helmholtz coils and the magnetic field that they create was determined. To do this, the respective spectral position of the CPT resonance was measured at different current values. These measurements were conducted in the approximation that the CPT resonance position is a linear function of the magnetic field strength. Such measurements were done for each axis independently. The coupling factor of the magnetic field and the Helmholtz coil current was found to be 244 nT/mA for the X axis, 279 nT/mA for the Y axis, and 216 nT/mA for the Z axis. The observed difference of this factor among the three axes arises from differences in the winding of the Helmholtz coils. The current sources were the PXIe-4145 (National Instruments). The noise of the current source is 100 nA; thus, the error caused by the current source was minimal.

The CPT resonance was scanned along each of the three coordinates to measure the magnitude and direction of the external magnetic field. Z-axis (parallel to the beam) scanning was done in frequency, whereas scanning along the other two coordinates (X, Y normal to the beam) was performed by adjustment of magnetic field arising from alternating current flowing through the corresponding Helmholtz coils. The resonance scanning along the Z axis was performed in frequency to avoid adding yet another AC magnetic field to the system, thus increasing interference. The position of the resonance corresponding to the Z axis was determined by the lock-in amplifier at the frequency of 2 kHz by modulating the frequency of the frequency synthesizer. Modulation frequencies of the resonance position corresponding to the X and Y axes were set at 1.5 and 1.7 kHz, respectively, by modulation of the current flowing through the corresponding coils. To do this, sine-wave signals were amplified using the current amplifiers and mixed with the DC current; the resulting current was fed to the coils. Different aliquant modulation frequencies were chosen to avoid interference. The difference and aliquancy of the modulation frequencies allowed using all the control loops at the same time to measure all three components of the magnetic field simultaneously. The resulting detuning from the resonances was compensated by current sources that control the currents fed to the Helmholtz coils (to X, Y, Z in Fig. 1). The current in each pair of the coils was proportional to the corresponding component of the measured magnetic field vector.

3. RESULTS

Figure 3 shows the sensitivity of the developed CPT vector magnetometer along different coordinates. It can be observed that the Z-axis sensitivity amounts to 300 pT/$\sqrt{\text{Hz}}$ at 10-Hz bandwidth, while the X- and Y-axes sensitivity was 400 and 300 pT/$\sqrt{\text{Hz}}$, respectively. The 10-Hz limitation was imposed by the capabilities of our apparatus. The integration time of the photodetector signal in the lock-in amplifier was 50 ms, which limited the bandwidth of the feedback control loops to 10 Hz. We believe that broadening of the frequency bandwidth is possible, but it will not likely lead to significant sensitivity improvement.

The difference in the magnetometer sensitivity along different axes comes, most probably, from different modulation methods and imperfect manual winding of Helmholtz coils.

It is important to point out that the data of Fig. 3 are given for a 10-Hz bandwidth. The magnetometer sensitivity should be even higher within narrower bands (<10 Hz), even though this needs additional research because technical noises tend to increase as the bandwidth becomes narrower.

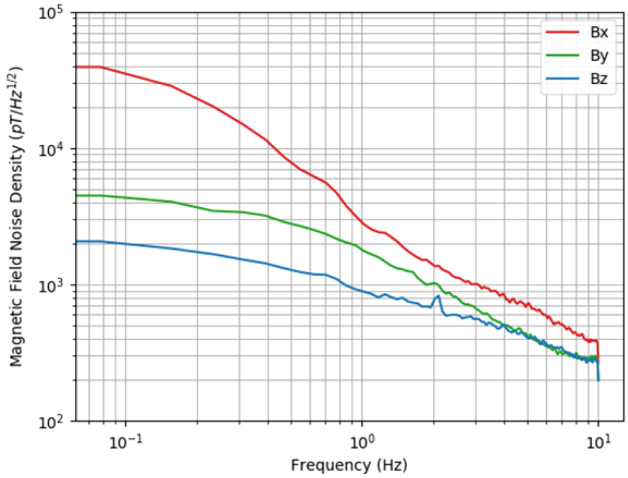

Fig. 3. Axial component sensitivity of the vector magnetometer. X-sensitivity corresponds to the red curve, Y — to the green curve, and Z — to the blue curve.

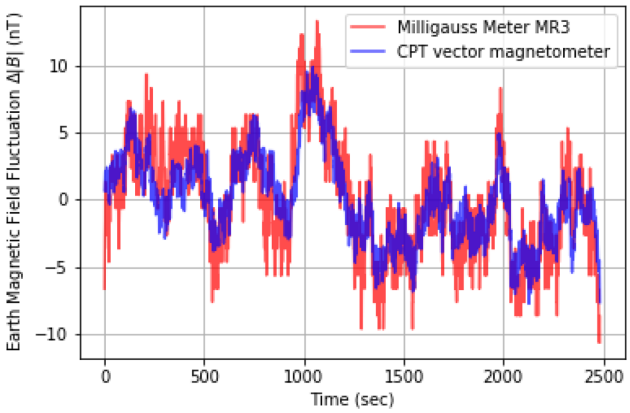

Fig. 4. Measurement of the Earth's magnetic field by the commercial magnetometer MR3 by AlphaLab Inc. (red trace) and the proposed CPT-based vector magnetometer (blue trace).

Tuning the developed CPT vector magnetometer consisted of calibrating the measured quantities governed by the relation $|B| = \sqrt{(B_x^2 + B_y^2 + B_z^2)}$. For this purpose, a commercial device by AlphaLab, Inc. was used (3-Axis Magnetoresistive Milligauss Meter MR3). The specified sensitivity of this device is 0.01 mG. Presented in Fig. 4 is a comparison of measurements of the Earth magnetic field taken with the studied CPT vector magnetometer and the commercial device. The commercial magnetometer was placed 10 cm above the studied system; therefore, their mutual interference may be neglected. The optical part of our system and the commercial magnetometer were placed inside the thermostat, significantly reducing the Earth's natural magnetic field. The thermostat is not an essential component for functioning of the magnetometer. In this case, it was used in order to eliminate the effect of ambient temperature fluctuations on the magnetometer stability. Figure 4 confirms that the developed CPT vector magnetometer measures the Earth magnetic field correctly.

It is necessary to note that the data in Fig. 4 are provided for demonstration of feasibility and sensitivity of the proposed magnetometer and do not refer to any calibration.

For measurement of the field direction, the data of Fig. 4 were expressed through angular parameters θ and φ, of which θ is the inclination or the angle between the Z axis (Fig. 1) of the magnetometer and the magnetic field direction, whereas φ is the azimuth or the angle between the X axis of the magnetometer and the projection of the magnetic field vector onto the XY plane. The respective dependencies are shown in Fig. 5. As it may be seen from Figs. 5(a) and 5(b), fluctuations of the magnetic field direction in the azimuthal coordinate are substantially smaller and comparable to the measurement noise. The magnitude of this noise is approximately 0.2 mrad, corresponding to magnetometer's angular resolution of $\sim 0.01°$. Essentially, the angular resolution limit of the proposed magnetometer is determined by the system noise floor. In this particular case, the fundamental limitation is set by the shot noise of the photodetector, which determines the signal/noise ratio of the spectroscopic signal. However, we believe, in general, that the major contribution to the noise floor comes from technical sources of noise, which may be reduced by proper engineering

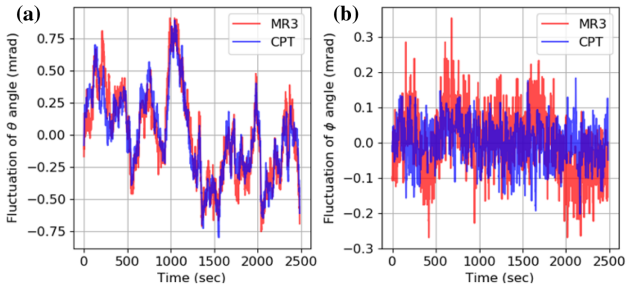

Fig. 5. Fluctuations of the direction of the Earth's magnetic field measured with the proposed magnetometer: (a) θ–inclination or the angle between the Z axis of the magnetometer (Fig. 1) and the magnetic field vector; (b) φ–azimuth or the angle between the X axis of the magnetometer and the projection of the magnetic field vector onto the XY plane.

(reduction of the device footprint, better shielding of the control electronics, etc.).

It is necessary to remark that an optical vector magnetometer with similar angular resolution and relatively small dimensions may be implemented on the basis of a different principle [30], the common factor among these attempts is to make a highly sensitive magnetometer using commercially available components as much as possible.

4. CONCLUSION

A CPT vector magnetometer can be easily created out of a CPT atomic clock with an additional system of 3D Helmholtz coils for compensation of the external magnetic field. Such a system does not have any moving parts. It allows measurement of the strength and direction of the external magnetic field at the sensitivity level of sub$-$nT/Hz$^{1/2}$ within a 10-Hz bandwidth. Angular resolution of the developed vector magnetometer amounts to about 10^{-2} degrees. Among the advantages of the proposed magnetometer are its fairly high sensitivity within small dimensions, the absence of blind spots, and compatibility with magnetic fields of broad strength range.

Funding. Russian Science Foundation (21-12-00057); Ministry of Science and Higher Education of the Russian Federation (FSUS-2020-0036).

Acknowledgment. Portions of this work were presented at the Photonics West conference in 2020, "Quantum vector magnetometer based on the CPT effect in ^{87}Rb vapour." The work of D. Radnatarov on implementation of the experimental installation was supported by the RSF. The work of V. Andryushkov and S. Kobtsev on generation and processing of the experimental data was supported by the Ministry of Science and Higher Education of the Russian Federation.

Disclosures. The authors declare no conflicts of interest.

Data availability. Data underlying the results presented in this paper are not publicly available at this time but may be obtained from the authors upon reasonable request.

REFERENCES

1. J. Kitching, "Chip-scale atomic devices," Appl. Phys. Rev. **5**, 031302 (2018).
2. J. Vavier, "Atomic clocks based on coherent population trapping: a review," Appl. Phys. B **81**, 421–442 (2005).
3. D. Budker and M. Romalis, "Optical magnetometry," Nat. Phys. **3**, 227–234 (2007).

4. D. Budker and D. Kimball, eds., *Optical Magnetometry* (Cambridge University, 2013).
5. R. Mhaskar, S. Knappe, and J. Kitching, "A low-power, high-sensitivity micromachined optical magnetometer," Appl. Phys. Lett. **101**, 241105 (2012).
6. R. Lutwak, D. Emmons, T. English, W. Riley, A. Duwel, M. Varghese, D. Serkland, and G. Peake, "The chip-scale atomic clock–recent development progress," in *Proceedings of the 35th Annual Precise Time and Time Interval Systems and Applications Meeting*, San Diego, California, December 2003, pp. 467–478.
7. A. Ludlow, M. Boyd, J. Ye, E. Peik, and P. Schmidt, "Optical atomic clocks," Rev. Mod. Phys. **87**, 637 (2015).
8. M. Romalis and H. Dang, "Atomic magnetometers for materials characterization," Mater. Today **14**(6), 258–262 (2011).
9. E. Alexandrov, M. Balabas Kulyasov, A. Ivanov, A. Pazgalev, J. Rasson, A. Vershovski, and N. Yakobson, "Three-component variometer based on a scalar potassium sensor," Meas. Sci. Technol. **15**, 918 (2004).
10. V. I. Yudin, A. V. Taichenachev, Y. O. Dudin, V. L. Velichansky, A. S. Zibrov, and S. A. Zibrov, "Vector magnetometry based on electromagnetically induced transparency in linearly polarized light," Phys. Rev. A **82**, 033807 (2010).
11. C. Affolderbach, M. Stähler, S. Knappe, and R. Wynands, "An all-optical, high-sensitivity magnetic gradiometer," Appl. Phys. B **75**, 605–612 (2002).
12. B. Patton, E. Zhivun, D. C. Hovde, and D. Budker, "All-optical vector atomic magnetometer," Phys. Rev. Lett. **113**, 013001 (2014).
13. L. Lenci, A. Auyuanet, S. Barreiro, P. Valente, A. Lezama, and H. Failache, "Vectorial atomic magnetometer based on coherent transients of laser absorption in Rb vapor," Phys. Rev. A **89**, 043836 (2014).
14. S. Pradhan, "Three axis vector atomic magnetometer utilizing polarimetric technique," Rev. Sci. Instrum. **87**, 093105 (2016).
15. W. Zheng, S. Su, G. Zhang, X. Bi, and Q. Lin, "Vector magnetocardiography measurement with a compact elliptically polarized laser-pumped magnetometer," Biomed. Opt. Express **11**, 649–659 (2020).
16. A. Papoyan, S. Shmavonyan, A. Khanbekyan, K. Khanbekyan, C. Marinelli, and E. Mariotti, "Magnetic-field-compensation optical vector magnetometer," Appl. Opt. **55**, 892–895 (2016).
17. S. Inglebya, P. Griffin, A. Arnold, M. Chouliara, and E. Riis, "High-precision control of static magnetic field magnitude, orientation, and gradient using optically pumped vapour cell magnetometry," Rev. Sci. Instrum. **88**, 043109 (2017).
18. S. J. Seltzer and M. V. Romalis, "Unshielded three-axis vector operation of a spin-exchange-relaxation-free atomic magnetometer," Appl. Phys. Lett. **85**, 4804–4806 (2004).
19. H. Huang, H. Dong, L. Chen, and Y. Gao, "Single-beam three-axis atomic magnetometer," Appl. Phys. Lett. **109**, 3–6 (2016).
20. J. Tang, Y. Zhai, L. Cao, Y. Zhang, L. Li, B. Zhao, B. Zhou, B. Han, and G. Liu, "High-sensitivity operation of a single-beam atomic magnetometer for three-axis magnetic field measurement," Opt. Express **29**, 15641–15652 (2021).
21. A. Nagel, L. Graf, A. Naumov, E. Mariotti, V. Biancalana, D. Meschede, and R. Wynands, "Experimental realization of coherent dark-state magnetometers," Europhys. Lett. **44**, 31–36 (1998).
22. V. Andryushkov, D. Radnatarov, and S. Kobtsev, "Highly sensitive compact optical magnetometer on the basis of an atomic clock," in *Conference on Lasers and Electro-Optics*, OSA Technical Digest (Optical Society of America, 2021), paper JTu3A.148.
23. H. Hong, S. Park, S. Lee, M. Heo, J. Park, T. Kim, H. Kim, and T. Kwon, "Chip-scale ultra-low field atomic magnetometer based on coherent population trapping," Sensors **21**, 1517 (2021).
24. G. Pati, R. Tripathi, R. Grewal, M. Pulido, and R. Depto, "Synchronous coherent population trapping and its magnetic spectral response in rubidium vapor," Phys. Rev. A **104**, 033116 (2021).
25. S. Khripunov, D. Radnatarov, and S. Kobtsev, "Atomic clock based on a coherent population trapping resonance in 87Rb with improved high-frequency modulation parameters," Proc. SPIE **9378**, 93780A (2015).
26. S. Kobtsev, D. Radnatarov, S. Khripunov, I. Popkov, V. Andryushkov, T. Steshchenko, V. Lunin, and Y. Zarudnev, "Feedback-controlled and digitally processed coherent population trapping resonance conversion in 87Rb vapour to high-contrast resonant peak," New J. Phys. **19**, 043016 (2017).
27. A. Pollinger, R. Lammegger, W. Magnes, C. Hagen, M. Ellmeier, I. Jernej, M. Leichtfried, C. Kürbisch, R. Maierhofer, R. Wallner, G. Fremuth, C. Amtmann, A. Betzler, M. Delva, G. Prattes, and W. Baumjohann, "Coupled dark state magnetometer for the China seismo-electromagnetic satellite," Meas. Sci. Technol. **29**, 095103 (2018).
28. L. Margalit, M. Rosenbluh, and A. Wilson-Gordon, "Coherent-population-trapping transients induced by a modulated transverse magnetic field," Phys. Rev. A **88**, 023827 (2013).
29. S. Kobtsev, S. Donchenko, S. Khripunov, D. Radnatarov, I. Blinov, and V. Palchikov, "CPT atomic clock with cold-technology-based vapour cell," Opt. Laser Technol. **119**, 105634 (2019).
30. G. Chatzidrosos, J. Rebeirro, H. Zheng, M. Omar, A. Brenneis, F. Stürner, T. Fuchs, T. Buck, R. Rölver, T. Schneemann, P. Blümler, D. Budker, and A. Wickenbroc, "Fiberized diamond-based vector magnetometers," Front. Photon. **2**, 732748 (2021).